Role of Fragility of the Glass Formers in the Yielding Transition under Oscillatory Shear - Supplemental Information

Roni Chatterjee,[1] Monoj Adhikari,[1] and Smarajit Karmakar[1]

[1] *Tata Institute of Fundamental Research, 36/P, Gopanpally Village, Serilingampally Mandal, Ranga Reddy District, Hyderabad 500046, Telangana, India*

S1. EQUILIBRATION OF THE LIQUID

As discussed in the main text, our initial configuration before shear deformation starts is obtained by equilibrating the liquid at a given temperature. Below, we show the mean squared displacement (MSD) and overlap function as functions of time to demonstrate that the liquid has reached to equilibrium.

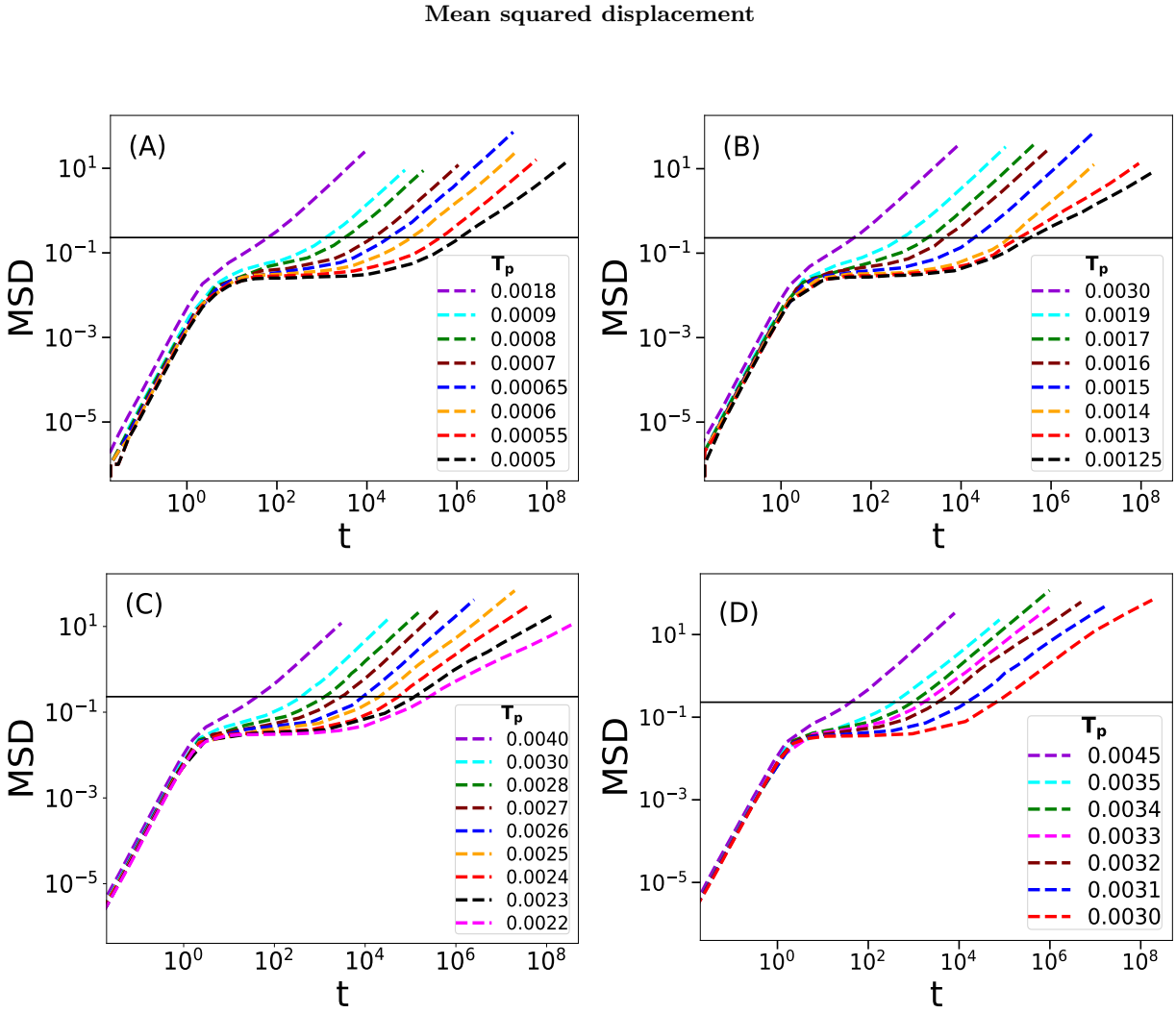

FIG. S1. Plot of mean squared displacement (MSD) with time t for system size N = 5000 at different parent temperatures (T_p) at densities (A) $\rho = 0.681$, (B) $\rho = 0.750$, (C) $\rho = 0.855$, (D) $\rho = 0.943$. The solid black line corresponds to the cut-off parameter $a^2 = 0.2304$.

Mean squared displacement (considering the B-type particles only) is defined as :

$$\Delta r^2(t) = \frac{1}{N_B} \sum_{i=1}^{N_B} |\vec{r_i}(t+t_0) - \vec{r_i}(t_0)|^2, \tag{S1}$$

where $r_i(t)$ is the position of the i-th particle at time t. The Mean Squared Displacement (MSD) is calculated by averaging over 12 samples. We have conducted long MD simulation runs (with a duration of approximately 10^8) to ensure that the MSD reaches the diffusive region for each temperature. The solid black line represents the value of the cut-off parameter $a^2 = 0.2304$, which we use to compute the overlap function, which is shown next.

Overlap function

The overlap function q(t) (considering the B-type particles only) is defined as :

$$q(t) = \frac{1}{N_B} \sum_{i=1}^{N_B} w\left(|\vec{r_i}(t_0) - \vec{r_i}(t+t_0)|\right) \tag{S2}$$

where $w(x) = 1.0$ if $x \leq a$ and $= 0$ otherwise. Here $a = 0.48$ is chosen from the plateau value ($a^2 = 0.2304$) of the MSD curves. q(t) is calculated by averaging over 12 samples. Again, the decay of $q(t)$ to zero ensures that we have equilibrated all the liquids at their respective temperatures. The relaxation time (τ_α) is calculated at the time where $q(t = \tau_\alpha) = \frac{1}{e}$.

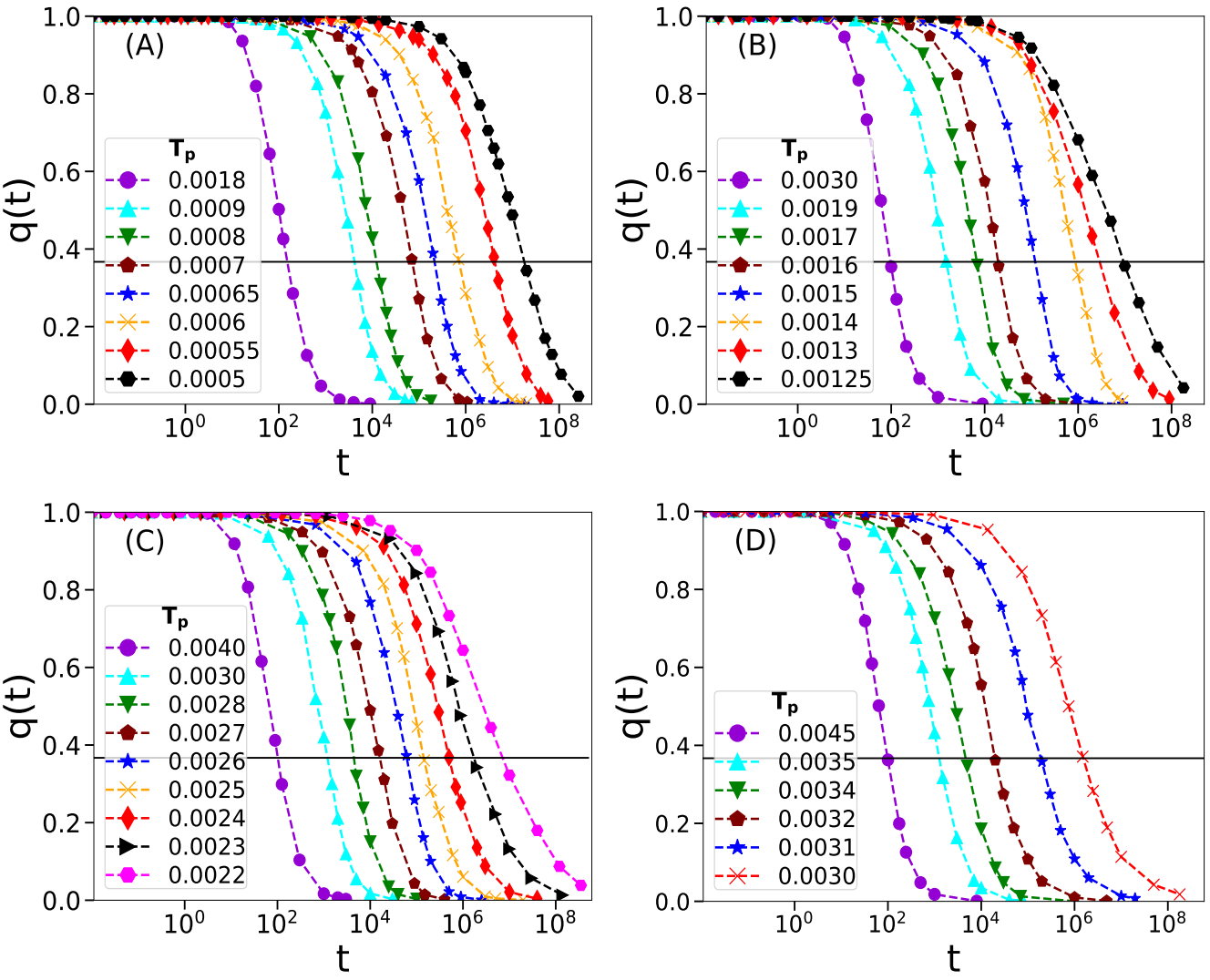

FIG. S2. Plot of overlap function q(t) with time t at wide range of parent temperatures (T_p) at densities (A) $\rho = 0.681$, (B) $\rho = 0.750$, (C) $\rho = 0.855$, (D) $\rho = 0.943$. The solid black line corresponds to $q(t = \tau_\alpha) = \frac{1}{e}$. System size N = 5000 for all panels.

S2. INHERENT STRUCTURE ENERGY

After equilibration, we achieve the amorphous solid state by minimizing the liquid. We employ the Conjugate Gradient method (CG) to minimize the liquid. These minimized configurations are referred to as inherent structure configurations. At low temperature region inherent structure energy (E_{IS}) varies with temperature (T) as : $E_{IS} = a - \frac{b}{T}$. Although this relation holds well at high density, this nature deviates for the lowest density $\rho = 0.681$. The fitted data (along with fitting parameters) are plotted for all densities. E_{IS} is calculated by averaging over 12 samples at each temperature and density.

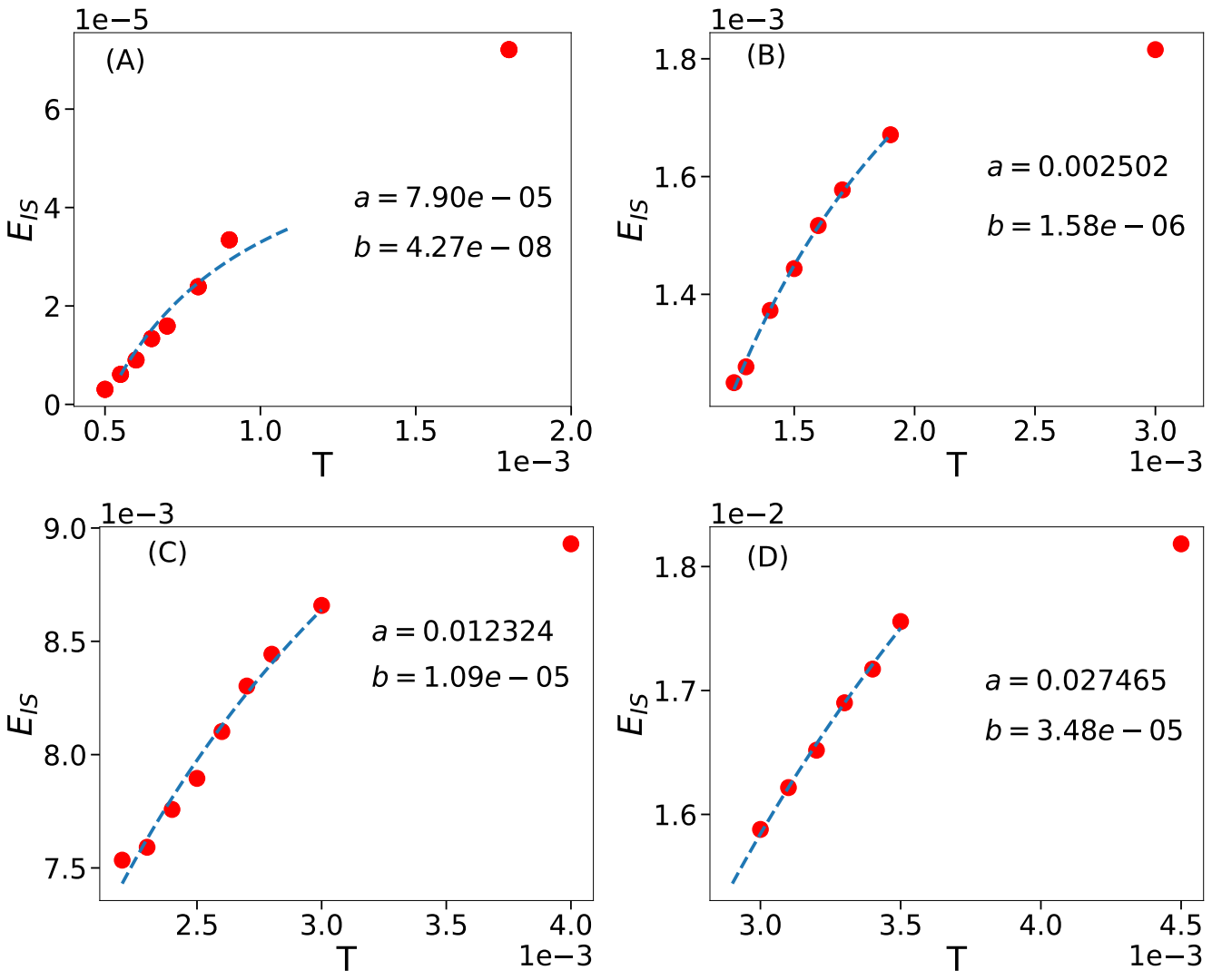

FIG. S3. Plot of inherent structure energy E_{IS} against temperature T for densities (A) $\rho = 0.681$, (B) $\rho = 0.750$, (C) $\rho = 0.855$, (D) $\rho = 0.943$. Each curve is fitted at low temperatures via the equation: $E_{IS} = a - b/T$. Only for the lowest density $\rho = 0.681$, E_{IS} shows deviation from $1/T$ behaviour.

S3. T_{MCT} FOR DIFFERENT DENSITY

As discussed in the main text, we observe a change in shear response behavior around the Mode Coupling temperature. Here, we show how we compute T_{MCT} for different densities. According to the Mode-Coupling theory, variation of relaxation time (τ_α) with temperatures (T) is well described by a power-law form: $\tau_\alpha = \tau_0(T - T_{MCT})^{-\gamma}$, where τ_α diverges at a critical temperature T_{MCT}. In Fig. S4, we illustrate τ_α of the liquids as a function of T at different density ρ along with MCT fits, and the corresponding fitted T_{MCT} is also indicated within the figures.

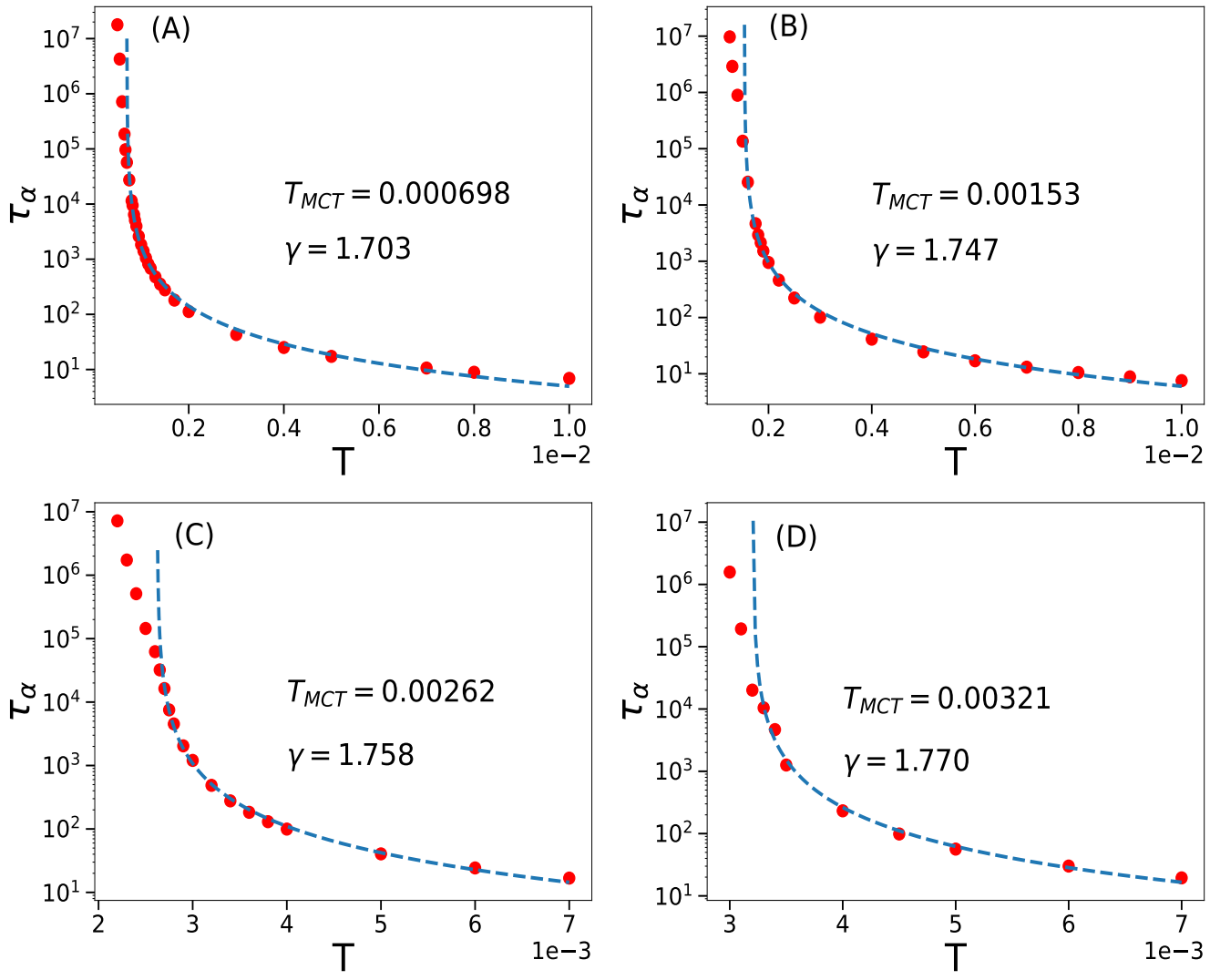

FIG. S4. Plots of τ_α extracted from the overlap function q(t), shown as a function of the temperature T on a semi-logarithmic scale, for densities (A) $\rho = 0.681$, (B) $\rho = 0.750$, (C) $\rho = 0.855$, (D) $\rho = 0.943$. Each curve is fitted by equation : $\tau_\alpha = \tau_0(T - T_{MCT})^{-\gamma}$. T_{MCT} is shown for all ρ for system size N = 5000.

S4. STROBOSCOPIC ENERGY WITH CYCLES AT DIFFERENT DENSITIES

Next, we show how the stroboscopic energy $E(\gamma = 0)$ evolves with the number of oscillatory shear cycles. Two extreme temperature cases — highest T (represents poorly annealed glass) and lowest T (represents well-annealed glass)—are considered within the studied temperature range for each ρ. Stroboscopic energy obtained from $T = 0.0018$ and $T = 0.0005$ at $\rho = 0.681$ are plotted for different values of strain amplitude (γ_{max}) in Fig S5. At the lowest density ($\rho = 0.681$), stroboscopic energies do not reach a perfect steady state even after thousands of cycles for a few γ_{max} in the poorly annealed case. Therefore, we fitted the E($\gamma = 0$) vs N_{cycle} data using the stretched exponential relation: $E(N_{cycle}) = E_0 + b\exp\left(-\left(\frac{N_{cycle}}{\tau}\right)^{\beta}\right)$ to extract the steady-state energies as well as the relaxation time, τ, representing the number of cycles to reach the steady state. The dashed lines represent the fitted data. From the fitting, we can extract τ, the relaxation time shown in the main text. Similarly, the variation of stroboscopic energies with cycles at different γ_{max} for the poorly annealed and well-annealed cases are also shown for $\rho = 0.750, 0.8556, 0.943$ in Fig. S6, S7, S8 respectively.

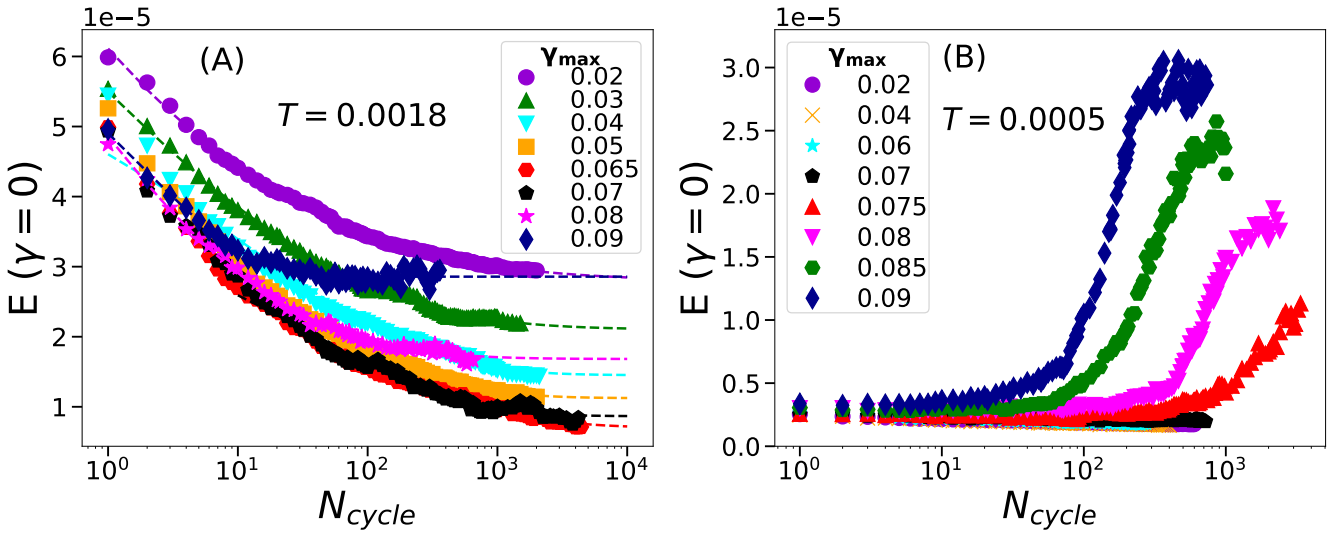

FIG. S5. Plot of stroboscopic energies with cycles at different γ_{max} at density $\rho = 0.681$ for (A) poorly annealed ($T = 0.0018$) and (B) well annealed ($T = 0.0005$). The data are averaged over 12 samples for the system size N = 5000. Dashed lines through the data set are fits to stretched exponential form. From fitting, we get the yield point is $\gamma_y \approx 0.065$ for the poorly annealed case. The yielding transition of the well-annealed sample is at $\gamma_y \approx 0.075$.

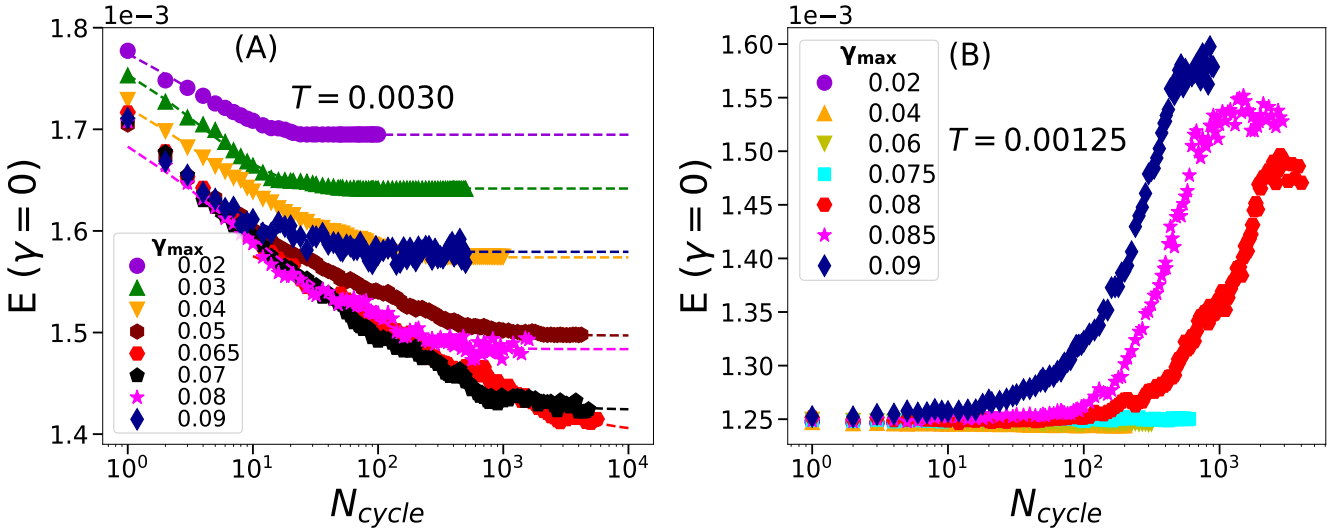

FIG. S6. Plot of stroboscopic energies with cycles at different γ_{max} at density $\rho = 0.750$ for (A) poorly annealed ($T = 0.0030$) and (B) well annealed ($T = 0.00125$). From fitting, we get the yield point of poorly annealed is at $\gamma_y \approx 0.065$. The yielding is at $\gamma_y \approx 0.08$ for the well-annealed case.

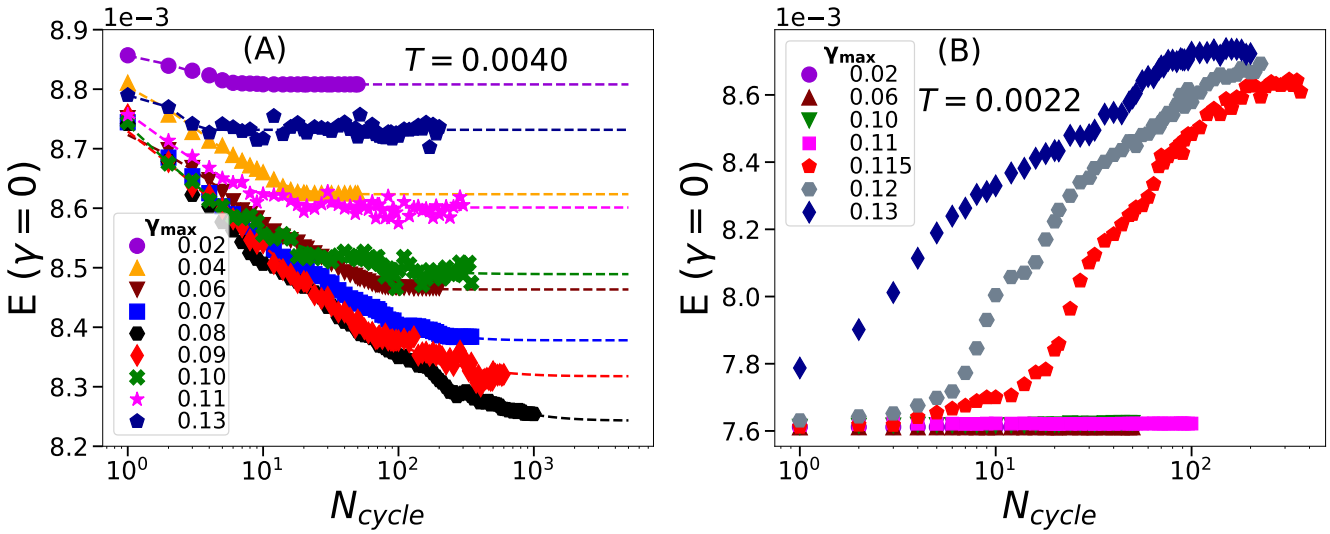

FIG. S7. Plot of stroboscopic energies with cycles at different γ_{max} at density $\rho = 0.855$ for (A) poorly annealed ($T = 0.0040$), (B) well annealed ($T = 0.0022$). The yield points of the poorly annealed and well-annealed cases are at $\gamma_y \approx 0.085$ and $\gamma_y \approx 0.115$, respectively.

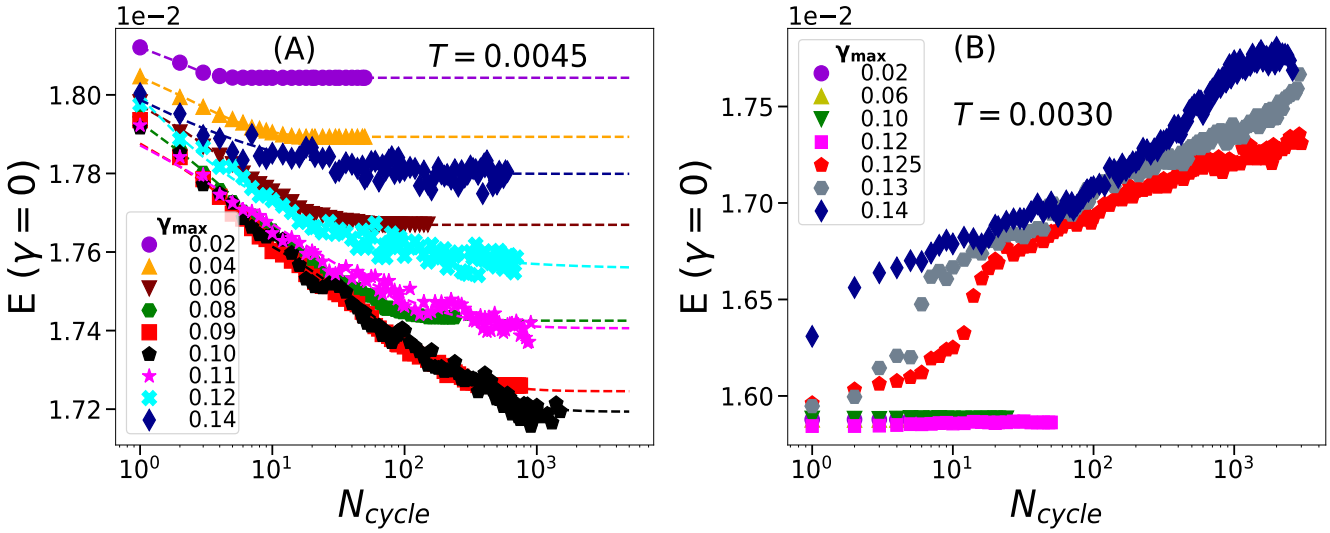

FIG. S8. Plot of stroboscopic energy vs cycles at different γ_{max} at density $\rho = 0.943$ for (A) poorly annealed ($T = 0.0045$), (B) well annealed ($T = 0.0030$) and their corresponding yielding is at $\gamma_y \approx 0.095$ and $\gamma_y \approx 0.125$ respectively.

S5. TIMESCALE TO REACH THE STEADY STATE

Now, we show the relaxation time, τ, obtained from the fitting described above as a function of $\gamma_{\max}$. As γ_{max} approaches the yield point γ_y, the relaxation time to reach the steady state diverges. Although various mechanisms have been proposed in the literature to explain how τ increases with $\gamma_{\max}$, we have observed that $\tau = a(\gamma_y - \gamma_{\max})^{-b}$ describes our data well. In Fig. S9, we show the relaxation time as a function of γ_{max} for different densities, where the dashed line represents the fit and the points represent the actual data from the simulation. Similar behaviour is also observed, as discussed in the main text for the elastoplastic model we studied. The corresponding data is shown in Fig. S10.

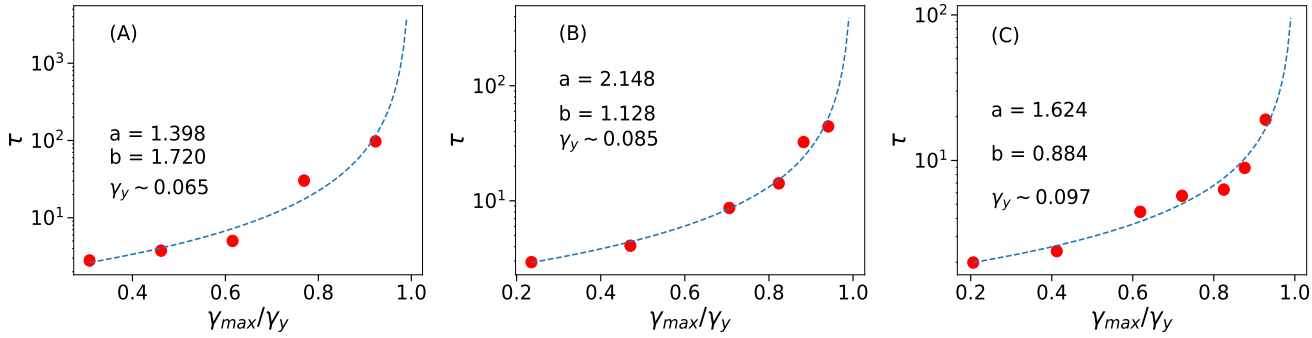

FIG. S9. Simulation: Relaxation time τ to reach the steady state for different γ_{max} for (A) $\rho = 0.750$, (B) $\rho = 0.855$, (C) $\rho = 0.943$. Red dots correspond to actual data, and the dashed lines are the fit to the data.

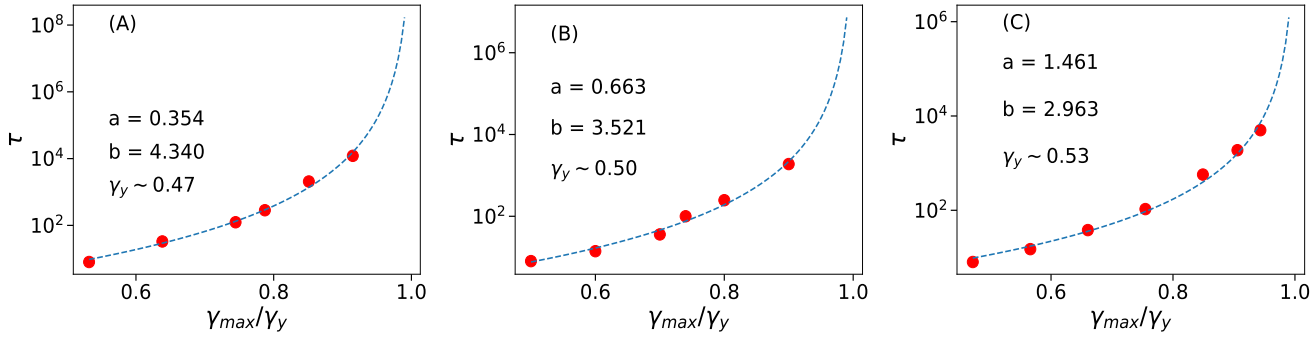

FIG. S10. Elastoplastic Model: Number of cycles required to reach the steady state for different γ_{max} for (A) strong, (B) intermediate, (C) fragile case. Red dots correspond to actual data, and the dashed lines are the fit to the data.